Role of Mitochondrial Dysfunction in Combined Bile Acid–Induced Cytotoxicity: The Switch Between Apoptosis and Necrosis

Anabela P. Rolo,* Carlos M. Palmeira,* Jon M. Holy,† and Kendall B. Wallace‡[,1]

*Center for Neurosciences and Cell Biology of Coimbra, Department of Zoology, University of Coimbra, 3004–517 Coimbra, Portugal; †Department of Anatomy and Cell Biology, University of Minnesota School of Medicine, 1035 University Drive, Duluth, Minnesota 55812; and ‡Department of Biochemistry and Molecular Biology, University of Minnesota School of Medicine, 1035 University Drive, Duluth, Minnesota 55812

The goal of this investigation was to determine whether chenodeoxycholic acid (CDCA)-induced apoptosis is prevented by ursodeoxycholic acid (UDCA) or tauroursodeoxycholic acid (TUDC) and to characterize the involvement of mitochondria in the process. Cultured human HepG2 cells were treated in a dose- and time-dependent protocol in order to establish a sufficiently low exposure to CDCA that causes apoptosis but not necrosis. Low-dose CDCA induced an S-phase block and G2 arrest of the cell cycle, as determined by flow cytometry. As a result, cell proliferation was inhibited. CDCA-induced apoptosis, as determined by fluorescence microscopy of Hoechst 33342-stained nuclei, was evident upon coincubation with TUDC. Additionally, after exposure to UDCA plus CDCA, the cell membrane was permeable to fluorescent dyes. Caspase-9-like activity, poly(ADP-ribose) polymerase (PARP) cleavage, and extensive DNA fragmentation were detected in CDCA-exposed cells and in cells coincubated with TUDC, but not UDCA. CDCA caused a decrease in mitochondrial membrane potential and depletion of ATP, both of which were potentiated by UDCA but not TUDC. The results suggest that UDCA potentiates CDCA cytotoxicity, probably at the level of induction of the mitochondrial permeability transition (MPT). Consequently, as suggested by the lack of the main hallmarks of the apoptotic pathway, in the presence of UDCA, CDCA-induced apoptosis is not properly executed but degenerates into necrosis.

Key Words: chenodeoxycholic acid; ursodeoxycholic acid; combination; apoptosis; necrosis; mitochondria.

Hydrophobic bile acids, such as chenodeoxycholic acid (CDCA), are implicated as major contributors to cholestatic liver diseases. Two mechanisms of cell death have been described: necrosis at high concentrations of bile acids and apoptosis at lower concentrations (Patel *et al.*, 1994; Spivey *et al.*, 1993).

[1] To whom correspondence should be addressed at Department of Biochemistry and Molecular Biology, University of Minnesota School of Medicine, 1035 University Drive, Duluth, MN 55812-2487. Fax: (218) 726-8014. E-mail: kwallace@d.umn.edu.

Previously, we have demonstrated that CDCA is toxic to hepatocytes by mechanisms involving mitochondrial dysfunction (Rolo *et al.*, 2003a). Furthermore, we demonstrated that ursodeoxycholic acid (UDCA) potentiates CDCA-induced necrosis in primary cultured hepatocytes (Rolo *et al.*, 2003b), by inducing the mitochondrial permeability transition (MPT). This adds to the growing controversy regarding the utility of UDCA in treating cholestatic diseases (Gores *et al.*, 1998; Krahenbuhl *et al.*, 1994; Rodrigues *et al.*, 1998).

In recent years, considerable research regarding the subject of cholestasis has focused on the mechanisms by which hydrophobic bile acids induce apoptosis, and the putative protective effect of UDCA. It has been suggested that bile acids induce cell death via ligand-dependent death receptor pathways, especially those involving the Fas receptor (Higuchi *et al.*, 2001; Miyoshi *et al.*, 1999). Other studies have implicated oxidative stress and mitochondrial dysfunction in bile acid–induced apoptosis (Graf *et al.*, 2002; Rodrigues *et al.*, 1998), specifically through induction of the MPT. Interestingly, hydrophobic and potentially toxic bile acids have been found to also activate survival pathways promoting cell proliferation (Qiao *et al.*, 2002; Rust *et al.*, 2000). The same survival pathway (activation of a mitogen-activated protein kinase, MAPK) has been implicated in protecting against UDCA toxicity, since UDCA has been shown to partially activate a pro-apoptotic cascade (Qiao *et al.*, 2002). It has been previously observed that UDCA induces apoptosis in hepatocellular carcinoma cells and potentiates photodynamic therapy (Kessel *et al.*, 2000; Oyama *et al.*, 2002).

The sum of these observations point to the necessity of systematic studies to fully understand the mechanisms of bile acids toxicity and the role of UDCA, either in preventing or potentiating bile acids toxicity. Toward this goal, we investigated whether CDCA-induced apoptosis is prevented by UDCA or its taurine-derivative, tauroursodeoxycholic acid (TUDC), and characterized the involvement of mitochondria in the process. Due to the interconnection between cell proliferation and programmed cell death, we also investigated the effects of bile acids on cell cycle.

MATERIALS AND METHODS

Materials. The human hepatoma cell line (HepG2) was obtained from American Type Culture Collection (ATCC, Rockville, MD). UDCA (97% purity) and CDCA (99% purity) were purchased from Sigma Chemical Co. (St. Louis, MO). TUDC, as sodium salt (97% purity), was purchased from Cal Biochem (La Jolla, CA). UDCA was dissolved in ethanol, TUDC and CDCA in water. Hoechst 33342, sulforhodamine B, and 5-bromo-2′-deoxyuridine (BrdU) were also purchased from Sigma (St. Louis, MO). Tetramethylrhodamine methyl ester (TMRM) and LIVE/DEAD Viability/Cytotoxicity Assay Kit were obtained from Molecular Probes (Eugene, OR). The DNA ladder molecular weight marker was from Promega (Madison, WI) and the BCA protein assay kit from Pierce Chemical (Rockford, IL). Caspase-9 synthetic substrate (Ac-LEHD-AFC) and specific inhibitor (Z-Leu-Glu/Ome)-His-Asp(Ome)-FMK.TFA inhibitor) were purchased from Enzyme Systems (Livermore, CA).

Purified mouse anti-BrdU and purified mouse anti-β-tubulin were purchased from Developmental Studies Hybridoma Bank (Iowa City, IA). Goat-anti-mouse Texas red was purchased from Jackson ImmunoResearch (West Grove, PA). Purified mouse anti-cytochrome c (clone 7H8.2C12) and purified mouse anti-human poly (ADP-ribose) polymerase (PARP, clone 4C10-5) were from PharMingen International (San Diego, CA). Goat anti-rabbit IgG was from Jackson ImmunoResearch Laboratories (West Grove, PA).

All other chemicals were of analytical grade and obtained from standard commercial sources.

Cell culture. HepG2 cells were cultured in Minimum Essential Medium (MEM) Eagle (with 2 mM L-glutamine and Earle's BSS adjusted to contain 1.5 g/l sodium bicarbonate, 0.1 mM nonessential amino acids, and 1 mM sodium pyruvate), containing 10% fetal bovine serum. Cells were maintained in a humidified CO_2 incubator at 37°C and passaged and harvested for experiments by detachment with 0.05% trypsin and 0.5 mM EDTA in phosphate-buffered saline (PBS); 80–90% confluent cells were used for bile acid treatment. Control cultures received an equivalent amount of vehicle (water or ethanol).

Cell proliferation assay. Cell proliferation was measured with sulforhodamine B as previously described (Skehan *et al.*, 1990). Briefly, cells were seeded in 24-well plates at 5×10^4 cells/ml and allowed to attach and recover for 1 day prior to drug treatment. After addition of bile acids at the concentrations indicated in the legends to the figures, cells were cultured for up to 3 days without media change or drug replenishment. At various time points, media was removed and the wells rinsed twice with cold PBS. Adherent cells were fixed with cold 10% trichloracetic acid on ice for 30 min, washed, and stained with 0.5 % sulforhodamine B. Absorbance of the solubilized dye was measured at 540 nm in a Shimadzu UV1201 spectrophotometer.

Viability assay. Cell viability was determined by the LIVE/DEAD Viability/Cytotoxicity Assay Kit (Papadopoulos *et al.*, 1994) by flow cytometry. At 24 or 48 h following exposure to 50 μM CDCA and/or 50 μM UDCA or TUDC, cells were harvested by trypsinization and washed twice with PBS. Cells were resuspended in the working solution of calcein-AM (2 μM) and ethidium homodimer-1 (Eth-D1; 4 μM) and incubated for 30 min at 37°C. The cells were then analyzed with a FACSCalibur flow cytometer (Becton Dickinson, San Jose, CA) and CELLQuest software. Approximately 10^5 cells were analyzed for each time point and treatment.

Nuclear apoptosis assay. HepG2 cell apoptosis was quantitated by determining the percentage of cells with nuclear morphologic changes of apoptosis detected by fluorescence microscopy of Hoechst 33342-stained fixed cells, as previously described (Holy, 2002). Briefly, cells were seeded on glass coverslips in 6-well plates at 5×10^4 cells/ml. At 24 or 48 h of treatment (50 μM CDCA and/or 50 μM UDCA or TUDC), coverslips were fixed and stored in formaldehyde and stained with 5 mg/ml Hoechst 33342. Coverslips were inspected and photographed on a Nikon Optiphot epifluorescence microscope using a Dage MTI SIT-68 video camera (Michigan City, IN). Two hundred and fifty cells from several randomly chosen fields were counted, and the number

of apoptotic cells was expressed as a percentage of the total number of cells counted.

Immunocytochemistry. Cells were seeded on glass coverslips in 6-well plates at 5×10^4 cells/ml. At 2 or 24 h of treatment (50 μM CDCA and/or 50 μM UDCA or TUDC), BrdU (5-bromo-2′-deoxyuridine) labeling solution (final concentration 10 μM in culture medium) was added and incubated for 3 h at 37°C. BrdU, a thymidine analogue, is a specific S-phase marker (Gratzner, 1982). Cells were then fixed and stored in cold (–10°C) absolute methanol. At 24 and 48 h of treatment (50 μM CDCA and/or 50 μM UDCA or TUDC), cells for labeling with antibodies to β-tubulin were also fixed. The procedure was essentially as previously described (Pierce *et al.*, 1999). Coverslips used for comparison of immunolabeling intensities between control and treated groups were all processed together and photographed at the same exposure times under identical conditions.

Cell cycle analysis. Cell cycle analysis based on DNA content was performed as follows. At 24 h, following exposure to experimental treatments (50 μM CDCA and/or 50 μM UDCA or TUDC), cells were harvested by trypsinization and washed twice with PBS. Cells were then suspended in PBS, and 100 μl of RNase (1 mg/ml) and 100 μl of propidium iodide (100 mg/ml) were added to the cell suspensions and incubated at 37°C for 30 min. The cells were then analyzed with a FACSCalibur flow cytometer (Becton Dickinson, San Jose, CA) and ModFit cell cycle analysis software. Approximately 10^5 cells were analyzed for each time point and treatment.

Detection of cytochrome c release in cells. To quantify cytochrome c release, immunoblot analysis of cytochrome c in the mitochondria and the cytosolic fractions were performed (Gottlieb and Granville, 2002). Briefly, at 48 h following exposure to experimental treatments (50 μM CDCA and/or 50 μM UDCA or TUDC), HepG2 cells were trypsinized, washed, and resuspended in 100 μl of ice-cold buffer (250 mM sucrose, 20 mM HEPES KOH (pH 7.5), 10 mM KCl, 1.5 mM $MgCl_2$, 1 mM EDTA, 1 mM DTT, 1 mM PMSF, 1 μg/ml aprotinin, and 1 μg/ml leupeptin). After 30 min incubation on ice, cells were homogenized with a glass Dounce homogenizer. The protein concentration in the cytosolic and mitochondrial fractions, upon separation by centrifugation, was detected using the BCA protein assay kit. Equal amounts of protein were resuspended in SDS–PAGE buffer and boiled in a water bath for 5 min. Lysates were stored at -80°C until further analysis. Proteins were separated under reducing conditions for 2 h at 120 V, as previously described (Pierce *et al.*, 1999).

Analysis of poly (ADP-ribose) polymerase cleavage. Poly (ADP-ribose) polymerase (PARP) cleavage was detected by Western blot. Briefly, at the end of treatment (48 h of exposure to 50 μM CDCA and/or 50 μM UDCA or TUDC), cells were collected by trypsinization and washed with PBS. The final cell pellet was resuspended in an approximately equal volume of Tris-buffered saline (TBS). A threefold volume of SDS sample buffer (6% sodium dodecyl sulfate, 5% b-mercaptoethanol, 0.01% bromophenol blue in 40% glycerol) was added and the mixture boiled for 10 min. The boiled sample was passed through a 28-gauge syringe multiple times to shear the DNA and stored at -80°C until assayed, as previously described (Pierce *et al.*, 1999).

Measurement of cellular caspase-9 activity. Caspase-9 activity was quantified by measuring cleavage of a fluorometric peptide Ac-LEHD-AFC. Briefly, at the end of designated treatments (48 h of exposure to 50 μM CDCA and/or 50 μM UDCA or TUDC), cells were harvested and washed with PBS, and equal numbers of control or treated cells were lysed in cell lysis buffer (10 mM Tris–HCl, pH 7.5, 10 mM NaH_2PO_4, 130 mM NaCl, 1% Triton X-100, and 10 mM NaPPi). The cell lysate was then incubated at 37°C with Ac-LEHD-AFC (10 μg/ml). After 2 h incubation, substrate cleavage leading to the release of the fluorescent AFC moiety (excitation 390 nm, emission 510 nm) was monitored by a Labsystems type 374 plate-reader. For blocking experiments, cell lysate was preincubated with caspase-9 specific inhibitor (Z-Leu-Glu/Ome-His-Asp(Ome)-FMK.TFA inhibitor) (10 μg/ml), prior to the addition of synthetic substrates. Changes in caspase activity were expressed as percent change from control, which was set as 100%.

Agarose electrophoresis for DNA fragmentation. Cells (1×10^6) collected after treatments (48 h of exposure to 50 μM CDCA and/or 50 μM UDCA or TUDC) were washed in ice-cold PBS and resuspended in 450 ml digestion buffer (100 mM NaCl, 10 mM Tris–HCl, pH 8, 25 mM EDTA, 0.5% SDS, 0.1 mg/ml proteinase K). RNase (final concentration 20 μg/ml) was then added, and incubation was continued at 37°C for 1 h. After incubation (50°C) overnight for complete digestion, DNA was extracted with an equal volume of phenol/chloroform/isoamyl alcohol and precipitated with ethanol. DNA fragmentation was detected by electrophoresis in 1.5% agarose gel containing 1 μg/ml ethidium bromide; 100-bp ladder molecular weight markers were used.

Measurement of mitochondrial membrane potential. To monitor mitochondrial transmembrane potential ($\Delta\psi$), HepG2 cells were loaded with 6.6 μM tetramethylrhodamine methyl ester (TMRM) in culture media, as previously described (Rolo *et al.*, 2003b). The different additions are shown in the legends to the figures.

Determination of ATP content. The extraction of ATP from cells was performed as previously described (Ryll and Wagner, 1991), after 48 h incubation of HepG2 cells in culture with the compounds (50 μM CDCA and/or 50 μM UDCA or TUDC). ATP was quantitated by HPLC as previously described (Stocchi *et al.*, 1985) and the concentration expressed per million viable cells as determined by Trypan blue exclusion.

Statistical analysis. Solvent controls (water or ethanol) were included within each experimental determination, and the numerical data are expressed as a percentage of the respective control (mean $\pm$ SEM, for 3–4 independent experiments). Ethanol itself had no effect on any of the parameters measured. Statistical significance was determined by the one-way ANOVA Student-Newman-Keuls post-*t*-test for multiple comparisons. A *p* value < 0.05 was considered statistically significant.

RESULTS

Effects on Cell Proliferation

In this work, cell proliferation was assessed as a fundamental parameter to determine time- and dose- dependent effects of bile acids (Fig. 1). Concentrations of 25, 50, 75, and 100 μM CDCA were evaluated for periods of 24, 48, and 72 h. Exposure of HepG2 cells to 25 μM CDCA had no effect on cell proliferation (data not shown). However, exposure to 50 μM CDCA for 24 h (data not shown) resulted in inhibition of cell proliferation that was even more pronounced at 48 h (Fig. 1).
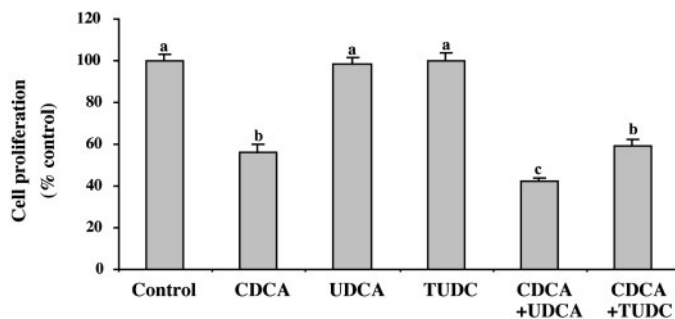
FIG. 1. Effects of bile acids (50 μM CDCA and/or 50 μM UDCA or 50 μM TUDC) on cell proliferation at 48 h. Cell proliferation was measured with sulforhodamine B. Percent proliferation was calculated by comparing with control cell proliferation, considered as 100% at each time point. Data represent the mean $\pm$ SEM of measurements of four separate experiments. Values that share the same letter are not statistically different (*p* < 0.05).
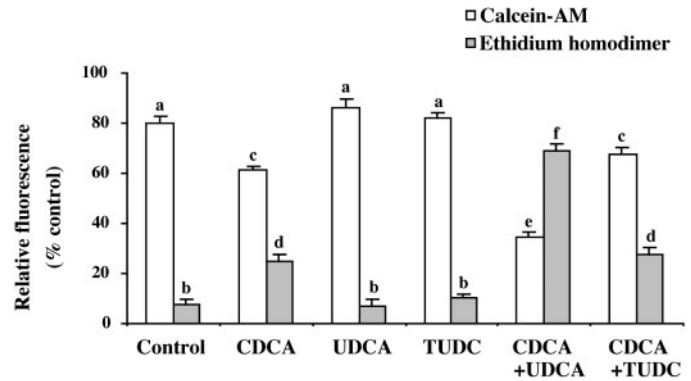
FIG. 2. Effects of bile acids on cell viability, based on retention of calcein-AM and ethidium homodimer in HepG2 cells, analyzed by flow cytometry. Cells were treated with 50 μM CDCA and/or 50 μM UDCA or 50 μM TUDC for 48 h. Alterations in probe retention were determined by flow cytometry. Percent probe retention was calculated by comparing with control probe retention, considered as 100%. Data represent the mean $\pm$ SEM of four separate experiments. Values that share the same letter are not statistically different (*p* < 0.05).

Since no cells were detached (an initial indicator of acute cell damage), we concluded that inhibition of cell proliferation was due to a specific effect of CDCA on cell division. A similar effect was observed at later time points (72 h) and at higher concentrations (75 and 100 μM) of CDCA (data not shown). Time- (24, 48 and 72 h) and dose- (25, 50, 75, and 100 μM) response studies for UDCA and TUDC revealed that these bile acids by themselves did not have any effect on HepG2 cell proliferation in culture (Fig. 1). However, upon coincubation with CDCA (50 μM) plus UDCA (50 μM) for 48 h, inhibition of cell proliferation was potentiated (Fig. 1). TUDC (50 μM) did not alter CDCA effects on cell proliferation.

Effects on Cell Viability

The next set of experiments was designed to confirm that, at the concentrations selected, bile acids did not elicit any alteration on plasma membrane integrity, which is an indicator of necrotic cell death. Based on the results of the first set of experiments, 50 μM CDCA, UDCA, and TUDC were selected as the concentrations for use in these studies. Following exposure to 50 μM of bile acids for 48 h, cells were stained with a combination of calcein-AM and ethidium homodimer and analyzed by flow cytometry.

At 24 h, no membrane alterations were observed (data not shown). However, at 48-h exposure to CDCA, there was a decrease in calcein-AM and an enhancement of Eth-D1 fluorescence (Fig. 2), indicating an increase in plasma membrane permeability. This was not surprising since it is known that, at late stages of apoptosis, plasma membrane becomes permeable. UDCA or TUDC (50 μM) alone had no effect (Fig. 2). However, UDCA potentiated the changes caused by CDCA, suggesting an extensive population of damaged cells (Fig. 2). TUDC did not alter the toxicity caused by CDCA (Fig. 2).

Effects on Cell Cycle

Cell cycle effects of CDCA were investigated in a series of experiments using the same protocol but two different assays (flow cytometry and microscopy). After 24-h exposure to the different compounds, cells were harvested and cell cycle analyzed (Figs. 3A and 3B). This time point was chosen because we have previously observed an inhibition of cell proliferation without changes in cell viability.

Exposure to CDCA for 24 h caused a marked decrease in the number of cells in S phase, suggesting an S-phase block and G2 arrest (Fig. 3A). UDCA and TUDC by themselves had no effect on cell cycle, nor did they alter cell cycle response to CDCA (Fig. 3A).

We performed an additional study to evaluate DNA synthesis, measuring bromodeoxyuridine (BrdU) incorporation (Fig. 3B, lower panel). Less then 1% of cells treated with 50 μM CDCA for 24 h incorporate BrdU. The 24-h exposure was compared with an earlier short (2 h) exposure to establish a time-dependent effect. We conclude that CDCA at 24 h induced cell growth inhibition through induction of cell cycle arrest, because no significant apoptosis is evident in these cell
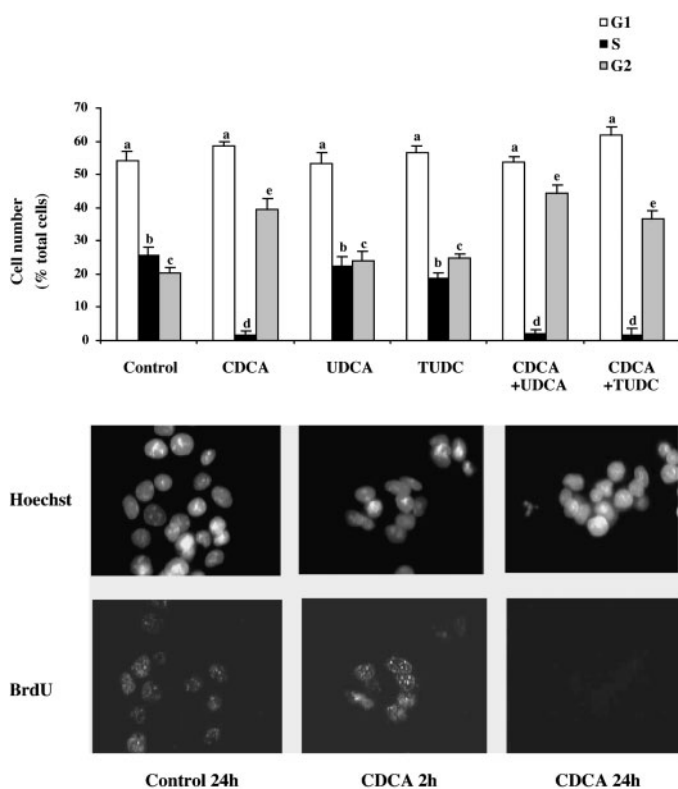

FIG. 3. (A) Effects on cell cycle of HepG2 cells by flow cytometry. Cells were treated with 50 μM CDCA and/or 50 μM UDCA or 50 μM TUDC for 24 h. Data represent the mean ± SEM of three separate measurements. Values that share the same letter are not statistically different ($p < 0.05$). (B) Micrographs showing cells treated for 2 h and 24 h with 50 μM CDCA. Cells were double-labeled with Hoechst 33342 for DNA (upper panel) and antibody to BrdU (lower panel).
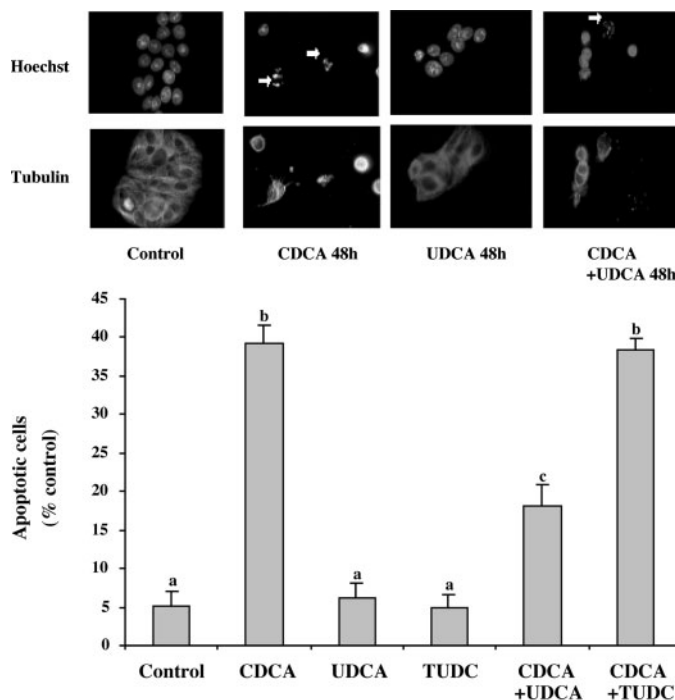

FIG. 4. (Top) Micrographs showing cells treated with 50 μM CDCA and/or 50 μM UDCA for 48 h. Cells were double-labeled with Hoechst 33342 for DNA (upper panel) and antibody to tubulin (lower panel). Arrows indicate apoptotic nuclei. (Bottom) Percentage apoptosis as determined by Hoechst 33342 staining. Cells were treated with 50 μM CDCA and/or 50 μM UDCA or 50 μM TUDC for 48 h. Percent apoptosis was obtained by comparing with control cell apoptosis, considered as 100% at time 0. Data represent the mean ± SEM of three separate experiments. Values that share the same letter are not statistically different ($p < 0.05$).

cultures as shown in Figure 3B (upper panel) with cells labeled with Hoechst 33342.

Effects on Chromatin Condensation and Tubulin Organization

In the sequence of the results described, we evaluated DNA changes by Hoechst 33342 staining following cell exposure to the different compounds for 48 h. Since apoptotic cells undergo a marked change in morphology, we also assessed alterations in tubulin organization, a component of the cytoskeleton.

A study of the nuclear changes, by staining with Hoechst 33342 dye, demonstrated that 50 μM CDCA induced nuclear changes typical of apoptosis in 40% of the cells by 48 h (Figs. 4A and 4B). Disorganization of tubulin was also observed (Fig. 4A).

The percentage of apoptotic nuclei upon combined exposure to both CDCA and TUDC did not differ from that in CDCA-treated cells (Fig. 4B). In contrast, treatment with 50 μM UDCA plus 50 μM CDCA resulted in fewer apoptotic nuclei (Fig. 4A). Taking into account the previous results in which a

rapid loss of plasma membrane integrity was observed under the same experimental conditions (Fig. 2), we propose that the decreased apoptosis indicates that these cells underwent necrosis. UDCA and TUDC by themselves did not stimulate apoptosis (Figs. 4A and 4B).

Effects on DNA Fragmentation

DNA fragmentation was used as another criterion to distinguish between apoptosis and necrosis. Consistent with the previous nuclear changes, cells treated with 50 μM CDCA or 50 μM CDCA plus 50 μM TUDC for 48 h started to show DNA fragmentation (Fig. 5). In UDCA plus CDCA–treated cells, on the other hand there was no cleavage of DNA that could be detected by gel electrophoresis (Fig. 5). No DNA fragmentation was observed in cells treated with UDCA or TUDC alone. These results further support a prominent role for necrotic cell death upon exposure to the combination UDCA plus CDCA, although apoptotic nuclei were observed with Hoechst 33342 staining.

Effects on Poly (ADP-Ribose) Polymerase (PARP)

We next assessed cleavage of the caspase-3 substrate PARP, another feature of apoptosis. Cleavage of PARP was observed in cells exposed to CDCA and TUDC plus CDCA, but not any other conditions (Fig. 6). The absence of PARP cleavage in cells exposed to CDCA plus UDCA further suggested that UDCA potentiates CDCA cytotoxicity through necrotic, rather then apoptotic cell death.
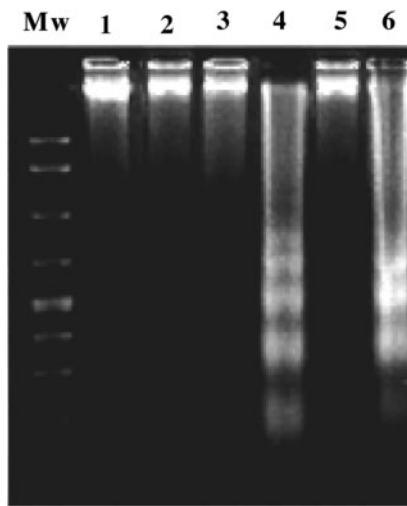

FIG. 5. Pattern of DNA fragmentation in HepG2 cells. Cells were incubated with 50 μM CDCA and/or 50 μM UDCA, TUDC for 48 h. DNA fragmentation was assayed on 1.5% agarose gels. Lane Mw, marker; lane 1, control; lane 2, UDCA; lane 3, TUDC; lane 4, CDCA; lane 5, CDCA + UDCA; lane 6, CDCA + TUDC.
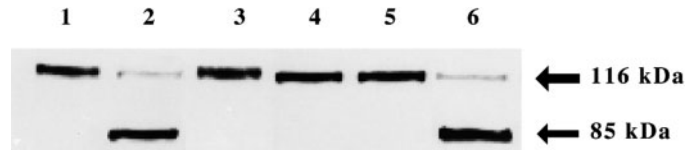

FIG. 6. The cleavage of caspase-3 substrate, PARP, during cell death. Cells were incubated with 50 μM CDCA and/or 50 μM UDCA or TUDC for 48 h. PARP cleavage was analyzed by Western blot. Lane 1, control; lane 2, CDCA; lane 3, UDCA; lane 4, TUDC; lane 5, CDCA + UDCA; lane 6, CDCA + TUDC.

Effects on Caspase-9 Activity

To determine whether mitochondria were involved in the observed apoptosis caused by CDCA, we evaluated caspase-9 activity. Figure 7 presents the effects of bile acids on activated caspase-9 activity. Fluorescence due to the release of the fluorescent AFC moiety upon cleavage of the peptide Ac-LEHD-AFC by caspase-9 increased dramatically in cells treated with CDCA or CDCA plus TUDC. The general caspase-9 specific inhibitor (Z-Leu-Glu/Ome)-His-Asp(Ome)-FMK.TFA inhibitor) prevented such increase in fluorescence. Although UDCA by itself did not change caspase-9 activity, it substantially inhibited caspase activation caused by CDCA (Fig. 7).

Effects on Cytochrome c Release

Release of cytochrome *c* is a key event in regulating caspase-3 activation by the apoptosome complex. We next assessed cytochrome *c* release in treated cells (Fig. 8). Cytochrome *c* release was detected after 24-h exposure to CDCA alone and in combination with UDCA or TUDC (data not shown), followed by a more marked release after 48 h. Indeed, upon 48-h treatment with 50 μM CDCA, results clearly demonstrate cytochrome *c* distribution in the cytoplasm in addition to mitochondrial localization, although mitochondrial fraction contained a considerably lower amount (Fig. 8). On the other
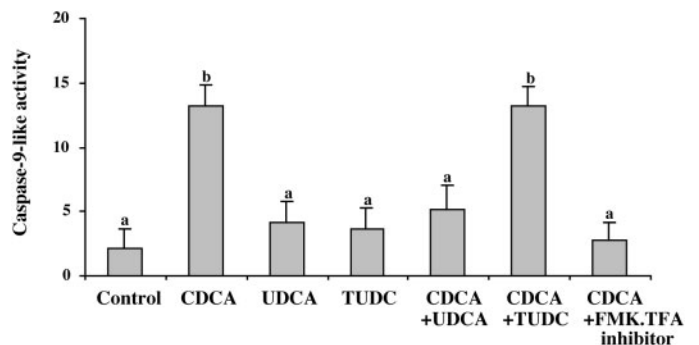

FIG. 7. Caspase-9 activation in HepG2 cells. Cells were incubated with 50 μM CDCA and/or 50 μM UDCA or TUDC for 48 h. Data represent the mean ± SEM of three separate experiments. Values that share the same letter are not statistically different ($p < 0.05$).

hand, in cells exposed to CDCA plus UDCA, cytochrome *c* was confined to the cytosolic fraction (Fig. 8). Coincubation with CDCA and TUDC did not affect the pattern of cytochrome *c* distribution as compared to cells incubated with CDCA alone (data not shown). After 48-h exposure to UDCA (Fig. 8) or TUDC, HepG2 cells retained cytochrome *c* in the mitochondrial fraction.

Effects on Mitochondrial Membrane Potential

To further analyze mitochondrial role in the process, we evaluated mitochondrial membrane potential ($\Delta\psi$) upon addition of bile acids (4 h) to cell suspensions. As shown in Figure 9, CDCA addition to HepG2 cells in suspension resulted in a decrease of TMRM retention (50%). UDCA by itself induced 15% depolarization. CDCA plus UDCA caused more substantial mitochondrial depolarization, when compared with CDCA alone. Cyclosporin A (CyA), a potent inhibitor of the mitochondrial permeability transition, prevented both CDCA and UDCA plus CDCA–induced depolarization of mitochondrial membrane potential (Fig. 9). Compared to cytochrome *c* release, which was observed upon 48 h of exposure to the compounds, mitochondrial depolarization occurs much earlier and before the release of cytochrome *c*.

Effects on ATP Content

In the previous reports, we have shown that exposure of cultured rat hepatocytes to bile acids results in decreased cellular ATP, which may reflect cell death due to bioenergetic failure (Rolo *et al.*, 2003b). The development of apoptosis requires ATP; a substantial loss of ATP contributes to inhibition of caspases (Eguchi *et al.*, 1999). We questioned whether maintenance of a critical ATP content is needed to prevent breakdown of the plasma membrane in CDCA-treated cells. Alternatively, cells exposed to the combination CDCA plus UDCA would have a premature demise to necrotic cell death due to ATP depletion. To pursue this, intracellular ATP content was measured in cells exposed to the bile acids for 48 h. As shown in Figure 10, exposure to CDCA caused a 25% decrease in cell ATP. Furthermore, coincubation with CDCA plus UDCA resulted in a dramatic 80% reduction in cellular ATP content. Addition of TUDC to CDCA-treated cells did not alter the effect of CDCA on cell ATP. UDCA and TUDC, alone, did not affect cell ATP.
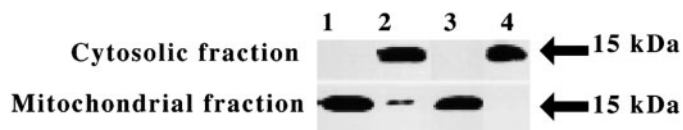
FIG. 9. Mitochondrial depolarization induced by bile acids (50 μM CDCA and/or 50 μM UDCA). In some experiments, cells were supplemented with 1 μM CyA. The change in $\Delta\Psi$ induced by the test agents was expressed as percent $\Delta\Psi$ in the absence of bile acids, taking into account the complete depolarization of mitochondrial membrane potential by FCCP. Data represent the mean $\pm$ SEM of three different measurements. Values that share the same letter are not statistically different ($p < 0.05$).

DISCUSSION

Apoptotic cell death induced by bile acids has emerged as an important mechanism underlying bile acid–induced hepatotoxicity. In this study, CDCA-induced apoptosis was associated with an initial block of S phase, the cell cycle phase in which cells are most sensitive to inhibitors of DNA synthesis. Inhibition of cell proliferation by conjugated and unconjugated bile

FIG. 10. Measurement of cellular ATP content after bile acids exposure. Cells were cultured in a glucose-free medium supplemented with 2 mM pyruvate and incubated with 50 μM CDCA and/or 50 μM UDCA or 50 μM TUDC for 48 h. Adenine nucleotides were determined by HPLC. Using this method, content for control cells was 82.5 $\pm$ 2.3 nmol/million cells. Data are expressed as percent content compared to untreated cells. Data represent the mean $\pm$ SE of three separate experiments. Values that share the same letter are not statistically different ($p < 0.05$).

FIG. 8. Cytochrome *c* release in HepG2 cells. Cells were incubated with 50 μM CDCA and/or 50 μM UDCA for 48 h. Cytochrome *c* release was analyzed by Western blot. Lane 1, control; lane 2, CDCA; lane 3, UDCA; lane 4, CDCA + UDCA.
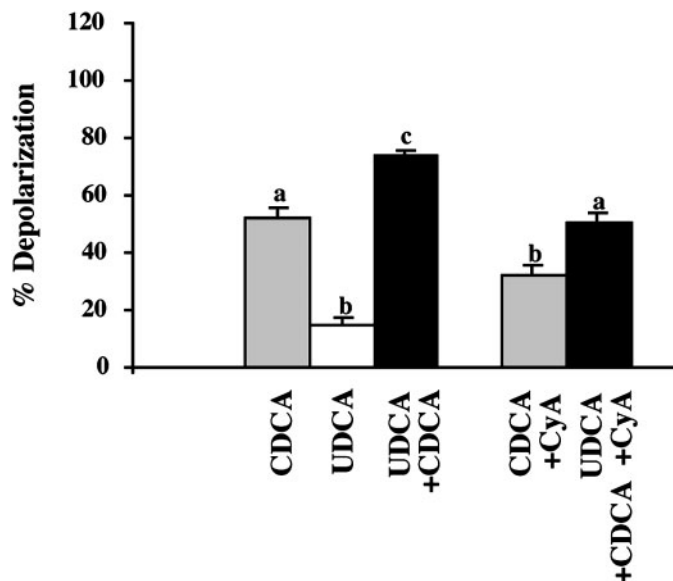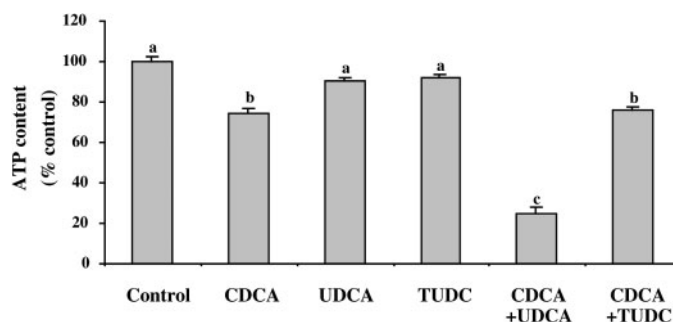
acids was also observed in rat hepatocytes in primary culture (Martinez-Diez *et al.*, 2000). The mechanism underlying CDCA inhibition of S phase was not addressed in this work. It is known that cell cycle regulators, such as p53, play an important role in the process of apoptosis (Kastan *et al.*, 1995). Since HepG2 cells have a wild-type p53, this might be one of the factors modulating the sensitivity to CDCA (Bressac *et al.*, 1990).

Numerous studies have demonstrated that cells undergoing apoptosis exhibit a decrease in mitochondrial membrane potential, preceding nuclear signs of apoptosis (Ferri and Kroemer, 2001), suggesting that early alterations of mitochondrial function may be important for initiating the apoptotic process. Our results demonstrate the activation of the mitochondrial apoptotic pathway in a hepatoma cell line following CDCA exposure, involving MPT induction. Such an event was shown by the early depolarization of mitochondrial membrane potential that is inhibited by CyA. In fact, impairment of mitochondrial function has previously demonstrated to be a key mechanism by which bile acids cause cell dysfunction (Krahenbuhl *et al.*, 1994; Rolo *et al.*, 2000, 2003b). Cytochrome *c* release and caspase-9 activation, with subsequent PARP cleavage and nuclear condensation, followed the onset of MPT by CDCA. It is well known that activated caspase-9 triggers a cascade that culminates in the activation of caspase-3, which cleaves several substrates, resulting in chromosomal DNA fragmentation and cellular morphologic changes characteristic of apoptosis (Cai *et al.*, 1998). Activation of caspase-9 usually occurs downstream of cytochrome *c* release from mitochondria and may be preceded by mitochondrial translocation of Bax (Narita *et al.*, 1998). A previous study by Rodrigues and coworkers, reported that deoxycholic acid–induced apoptosis in primary rat hepatocytes was associated with decreased mitochondrial transmembrane potential and increased mitochondria-associated Bax protein (Rodrigues *et al.*, 1999). Indeed, Bax activation has been proposed as an integrator of diverse pro- and anti-apoptotic signals, cell fate being decided by the resultant release of cytochrome *c* (Brenner and Kroemer, 2000). This would explain the role for the Fas pathway as a common mechanism by which cytotoxic bile acids also induce apoptosis (Sodeman *et al.*, 2000), which was not evaluated in the present work. Interestingly, a recent work by Schoemaker and coworkers (Schoemaker *et al.*, 2003) has shown that the glycine derivative of CDCA induces apoptosis in a mitochondria-controlled pathway in which caspase-8 is activated in a FADD-independent manner. Therefore, apoptotic pathways are differentially activated by the distinct bile acids.

From this study, UDCA potentiates MPT induction in HepG2 cells by CDCA, as previously shown in isolated mitochondria (Rolo *et al.*, 2000). The ability of UDCA to enhance mitochondrial membrane depolarization, sensitive to CyA, was associated with a much greater loss of ATP. Apoptotic changes in CDCA-treated cells occurred without a massive disruption of the plasma membrane as indicated by calcein-AM retention,

Eth-D1 exclusion, and ATP loss. Thus, it appears that apoptosis is activated at low CDCA concentration and occurs after a long time of exposure, when compared with the combined bile acid cytotoxicity. Interestingly, cells exposed to UDCA alone underwent only a slight decrease in mitochondrial membrane potential with no significant change in ATP content, suggesting that cytotoxicity induced by UDCA is only expressed when CDCA is present. Such an effect may occur by potentiation of MPT induction. One explanation for this difference could be that induction of the MPT in a small fraction of mitochondria could activate the apoptotic process, whereas induction of mitochondrial transition in a large portion of mitochondria could cause bioenergetic collapse, as shown by ATP depletion, beyond which apoptosis could not proceed, leading to necrosis. Previously, we have shown that CDCA plus UDCA induces a decrease in mitochondrial respiration and activates the mitochondrial permeability transition (Rolo *et al.*, 2000, 2003b), resulting in a bioenergetic failure, with cell death showing necrotic characteristics (Rolo *et al.*, 2003b). These changes occurred over a rapid time course (4 h) and following exposure to higher concentrations of bile acids (Rolo *et al.*, 2003b).

It has been proposed that caspase inactivation in lethally injured cells switches the mode of cell death from apoptosis to necrosis (Lemaire *et al.*, 1998). Although cytochrome *c* release in CDCA plus UDCA–treated cells was evident, no caspase activity was observed. Such results suggest that ATP depletion plays a key role in caspase inactivation and loss of plasma membrane integrity. It may also explain the inhibition of other typical features of apoptosis in cells exposed to CDCA plus UDCA.

It is clear that bile acids, although at higher concentrations than used in this work, stimulate the generation of reactive oxygen species in isolated rat hepatocytes, primary cultured hepatocytes, and purified hepatocyte mitochondria (Rodrigues *et al.*, 1998; Sokol *et al.*, 1995). Yerushalmi and collaborators reported that, in glycochenodeoxycholic acid–induced apoptosis, oxidative stress was a key mediator of the mitochondrial permeability transition (Yerushalmi *et al.*, 2001). We do not exclude the oxidation of cysteine residues in caspases as the mechanism responsible for their inactivation.

The role of UDCA in hepatic apoptosis is controversial. On one hand, UDCA has been described as decreasing apoptosis induced by deoxycholic acid and tumor growth factor-β in both hepatic and nonhepatic cells (Rodrigues *et al.*, 1998, 1999). The probable mechanism was suggested to be via modulation of mitochondrial function and membrane stability, although a role of alteration of the bile acid pool was not ruled out (Rodrigues *et al.*, 1998). Other authors have described potentiation of cell dysfunction induced by UDCA. UDCA induces apoptosis in hepatocellular carcinoma cells, mediated by increased levels of Bax in mitochondria and cytochrome *c* in the cytosol (Oyama *et al.*, 2002). Preincubation of murine leukemia and hepatoma cells with UDCA potentiated the effects of photodynamic therapy (Kessel *et al.*, 2000). Such action in-

volved effects at the level of mitochondrial depolarization, release of cytochrome *c* into the cytosol, and activation of caspase-3. Glyco- and tauro-conjugates of UDCA displayed the same action (Kessel *et al.*, 2000). In contrast, TUDC proved to be effective in reducing both GCDC-induced apoptosis and cytolysis (Benz *et al.*, 1998). The condition that UDCA exerts such an effect, if present before but not upon irradiation (Kessel *et al.*, 2000), supports our suggestion that UDCA per se does not cause mitochondrial membrane damage but lowers the threshold for the action of other compounds. Another interesting finding was the observation that UDCA activates a pro-apoptotic cascade, which is generally inhibited by a simultaneous and stronger activation of the MAPK survival pathway (Qiao *et al.*, 2002). These discrepant results may also be dependent on the different characteristics of the cell culture and the different expression of regulatory proteins. For example, S-adenosylmethionine has been described as an anti-apoptotic agent in cultured rat hepatocytes but pro-apoptotic in human hepatoma cells (Ansorena *et al.*, 2002).

Interestingly, besides a key regulatory role in signal transduction pathways, anti-apoptotic properties attributed to TUDC have been associated with potent mitochondrial membrane-stabilizing effects, preventing the binding of Bax to the outer mitochondrial membrane (Rodrigues *et al.*, 2001). However, previous studies with the goal to characterize the common apoptotic signaling pathways in human hepatoma cells have shown that p53 and c-Myc play a more important role in the apoptotic signaling pathway in HepG2 cells than the Bcl-2 gene family (Jiang *et al.*, 1996). Therefore, the lack of effect of TUDC in CDCA-induced apoptosis may be the result of activation of different apoptotic pathways. However, since the hepatoblastoma cell line HepG2 is unable to take up bile acids via sodium-dependent pathways (the main system for the uptake of conjugated bile acids) because Ntcp is not expressed (Boyer *et al.*, 1993), this may also be the explanation for TUDC behavior in this model. Sodium-independent hepatocellular uptake of bile salts is mediated by several members of the OATP family of membrane transporters, which are multispecific transporters that mediate hepatocellular uptake of a vast variety of other amphipathic organic compounds in HepG2 cells.

TUDC is the taurine conjugate of UDCA, and differential effects on the induction of apoptosis may be a consequence of the altered physical-chemical properties. For example, amidation is known to significantly reduce the cytotoxicity of the more lipophilic forms of unconjugated bile acids, both in hepatocytes (Scholmerich *et al*, 1984) and bile duct cells. Sarbu and coworkers (2001) published on the lipophilic character of bile acids and their tauro-conjugates and showed that the main difference between these compounds is their polarity and acidity. Tauro-conjugates are more polar and acidic and, thereby, substantially less lipophilic than unconjugated bile acids, which appear to be important determinants of cytotoxicity.

In summary, the results of this study demonstrate that activation of apoptosis by CDCA involves an early loss of mitochondrial membrane potential. Cytochrome *c* release and activation of the caspase cascade probably follow this initial event. Coincubation with UDCA appears to induce necrosis as the predominant form of cell death, by a mechanism that involves extensive mitochondrial dysfunction. In view of this, although CDCA, by itself and at low concentrations, is an inducer of apoptosis, UDCA potentiates CDCA cell toxicity not by increasing apoptosis, but by diverging to necrotic pathways.

ACKNOWLEDGMENTS

REFERENCES

Ansorena, E., Garcia-Trevijano, E. R., Martinez-Chantar, M. L., Huang, Z. Z., Chen, L., Mato, J. M., Iraburu, M., Lu, S. C., and Avila, M. A. (2002). S-adenosylmethionine and methylthioadenosine are antiapoptotic in cultured rat hepatocytes but proapoptotic in human hepatoma cells. *Hepatology* **35,** 274–280.

Benz, C., Angermuller, S., Tox, U., Kloters-Plachky, P., Riedel, H. D., Sauer, P., Stremmel, W., and Stiehl, A. (1998). Effect of tauroursodeoxycholic acid on bile-acid-induced apoptosis and cytolysis in rat hepatocytes. *J. Hepatol.* **28,** 99–106.

Boyer, J. L., Hagenbuch, B., Ananthanarayanan, M., Suchy, F., Stieger, B., and Meier, P. J. (1993). Phylogenic and ontogenic expression of hepatocellular bile acid transport. *Proc.Natl. Acad. Sci. U.S.A.* **90,** 435–438.

Brenner, C., and Kroemer, G. (2000). Apoptosis. Mitochondria–the death signal integrators. *Science* **289,** 1150–1151.

Bressac, B., Galvin, K. M., Liang, T. J., Isselbacher, K. J., Wands, J. R., and Ozturk, M. (1990). Abnormal structure and expression of p53 gene in human hepatocellular carcinoma. *Proc. Natl. Acad. Sci. U.S.A.* **87,** 1973–1977.

Cai, J., Yang, J., and Jones, D. P. (1998). Mitochondrial control of apoptosis: The role of cytochrome *c*. *Biochim. Biophys. Acta* **1366,** 139–149.

Eguchi, Y., Srinivasan, A,. Tomaselli, K. J., Shimizu, S., and Tsujimoto, Y. (1999). ATP-dependent steps in apoptotic signal transduction. *Cancer Res.* **59,** 2174–2181.

Ferri, K. F., and Kroemer, G. (2001). Mitochondria–the suicide organelles. *Bioessays* **23,** 111–115.

Gores, G. J., Miyoshi, H., Botla, R., Aguilar, H. I., and Bronk, S. F. (1998). Induction of the mitochondrial permeability transition as a mechanism of liver injury during cholestasis: A potential role for mitochondrial proteases. *Biochim. Biophys. Acta* **1366,** 167–175.

Graf, D., Kurz, A. K., Reinehr, R., Fischer, R., Kircheis, G., and Haussinger, D. (2002). Prevention of bile acid-induced apoptosis by betaine in rat liver. *Hepatology* **36,** 829–839.

Gratzner, H. G. (1982). Monoclonal antibody to 5-bromo- and 5-iododeoxyuridine: A new reagent for detection of DNA replication. *Science* **218,** 474–475.

Higuchi, H., Bronk, S. F., Takikama, Y., Werneburg, N., Takimoto, R, El-Deiry, W., and Gores, G. J. (2001). The bile acid glycochenodeoxycholate induces trail-receptor 2/DR5 expression and apoptosis. *J. Biol. Chem.* **276,** 38610–38618.

Gottlieb, R. A., and Granville, D. J. (2002). Analyzing mitochondrial changes during apoptosis. *Methods* **26,** 341–347.

Holy, J. M. (2002). Curcumin disrupts mitotic spindle structure and induces micronucleation in MCF-7 breast cancer cells. *Mutat. Res.* **518,** 71–84.

Jiang, M. C., Yang-Yen, H. F., Lin, J. K., and Yen, J. J. (1996). Differential regulation of p53, c-Myc, Bcl-2 and Bax protein expression during apoptosis induced by widely divergent stimuli in human hepatoblastoma cells. *Oncogene* **13,** 609–616.

Kastan, M. B., Canman, C. E., and Leonard, C. J. (1995). P53, cell cycle control and apoptosis: Implications for cancer. *Cancer Metastasis Rev.* **14,** 3–15.

Kessel, D., Caruso, J. A., and Reiners, J. J., Jr. (2000). Potentiation of photodynamic therapy by ursodeoxycholic acid. *Cancer Res.* **60,** 6985–6988.

Krahenbuhl, S., Fischer, S., Talos, C., and Reichen, J. (1994). Ursodeoxycholate protects oxidative mitochondrial metabolism from bile acid toxicity: Dose-response study in isolated rat liver mitochondria. *Hepatology* **20,** 1595–1601.

Lemaire, C., Andreau, K., Souvannavong, V., and Adam, A. (1998). Inhibition of caspase activity induces a switch from apoptosis to necrosis. *FEBS Lett.* **425,** 266–270.

Martinez-Diez, M. C., Serrano, M. A., Monte, M. J., and Marin, J. J. (2000). Comparison of the effects of bile acids on cell viability and DNA synthesis by rat hepatocytes in primary culture. *Biochim. Biophys. Acta* **1500,** 153–160.

Miyoshi, H., Rust, C., Roberts, P. J., and Gores, G. J. (1999). Hepatocyte apoptosis after bile duct ligation in the mouse involves Fas. *Gastroenterology* **117,** 669–677.

Narita, M., Shimizu, S., Ito, T., Chittenden, T., Lutz, R. J., Matsuda, H., and Tsujimoto, Y. (1998). Bax interacts with the permeability transition pore to induce permeability transition and cytochrome *c* release in isolated mitochondria. *Proc. Natl. Acad. Sci. U.S.A.* **95,** 14681–14686.

Oyama, K., Shiota, G., Ito, H., Murawaki, Y., and Kawasaki, H. (2002). Reduction of hepatocarcinogenesis by ursodeoxycholic acid in rats. *Carcinogenesis* **23,** 885–892.

Papadopoulos, N. G., Dedoussis, G. V., Spanakos, G., Gritzapis, A. D., Baxevanis, C. N., and Papamichail, M. (1994). An improved fluorescence assay for the determination of lymphocyte-mediated cytotoxicity using flow cytometry. *J. Immunol. Methods* **177,** 101–111.

Patel, T., Bronk, S. F., and Gores, G. J. (1994). Increases of intracellular magnesium promote glycodeoxycholate-induced apoptosis in rat hepatocytes. *J. Clin. Invest.* **94,** 2183–2192.

Pierce, T., Worman, H. J., and Holy, J. (1999). Neuronal differentiation of NT2/D1 teratocarcinoma cells is accompanied by a loss of lamin A/C expression and an increase in lamin B1 expression. *Exp. Neurol.* **157,** 241–250.

Qiao, L., Yacoub, A., Studer, E., Gupta, S., Pei, X., Grant, S., Hylemon, P. B., and Dent, P. (2002). Inhibition of the MAPK and PI3K pathways enhances UDCA-induced apoptosis in primary rodent hepatocytes. *Hepatology* **35,** 779–789.

Rodrigues, C. M., Fan, G., Ma, X., Kren, B. T., Steer, C. J. (1998). A novel role for ursodeoxycholic acid in inhibiting apoptosis by modulating mitochondrial membrane perturbation. *J. Clin. Invest.* **101,** 2790–2799.

Rodrigues, C. M., Ma, X., Linehan-Stieers, C., Fan, G., Kren, B. T., and Steer, C. J. (1999). Ursodeoxycholic acid prevents cytochrome c release in apoptosis by inhibiting mitochondrial membrane depolarization and channel formation. Cell Death Differ. 6, 842–854.

Rodrigues, C. M., Sola, S., Brito, M. A., Brondino, C. D., Brites, D., and

Moura, J. J. (2001). Amyloid beta-peptide disrupts mitochondrial membrane lipid and protein structure: Protective role of tauroursodeoxycholate. *Biochem. Biophys. Res. Commun.* **281,** 468–474.

Rolo, A. P., Oliveira, P. J., Moreno, A. J. M., and Palmeira, C. M. (2000). Bile acids affect liver mitochondrial bioenergetics: Possible relevance for cholestasis therapy. *Toxicol. Sci.* **57,** 177–185.

Rolo, A. P., Oliveira, P. J., Moreno, A. J. M., and Palmeira, C. M. (2003a). Chenodeoxycholate induction of mitochondrial permeability transition pore is associated with increased membrane fluidity and cytochrome *c* release: Protective role of carvedilol. *Mitochondrion* **2,** 305–311.

Rolo, A. P., Palmeira, C. M., and Wallace, K. B. (2003b). Mitochondrially mediated synergistic cell killing by bile acids. *Biochim. Biophys. Acta* **1637,** 127–132.

Rust, C., Karnitz, L. M, Paya, C. V., Moscat, J., Simari, R. D., and Gores, G. J. (2000). The bile acid taurochenodeoxycholate activates a phosphatidylinositol 3-kinase-dependent survival signaling cascade. *J. Biol. Chem.* **275,** 20210–20216.

Ryll, T., and Wagner, R. (1991). Improved ion-pair high-performance liquid chromatographic method for the quantification of a wide variety of nucleotides and sugar-nucleotides in animal cells. *J. Chromatogr.* **570,** 77–88.

Sarbu, C., Kuhajada, K., and Keveresan, S. (2001). Evaluation of the lipophilicity of the bile acids and their derivatives by thin-layer chromatography and principal component analysis. *J. Chromatogr. A* **917,** 361–366.

Schoemaker, M. H., Gommans, W. M., de la Rosa, L. C., Homan, M., Klok, P., Trautwein, C., van Goor, H., Poelstra, K., Haisma, H. J., Jansen, P. L., *et al.* (2003). Resistance of rat hepatocytes against bile acid-induced apoptosis in cholestatic liver injury is due to nuclear factor-kappa B activation. *J. Hepatol.* **39,** 153–61.

Scholmerich, J., Becher, M. S., Schmidt, K., Schubert, R., Kremer, B., Feldhaus, S., and Gerok, W. (1984). Influence of hydroxylation and conjugation of bile salts on their membrane-damaging properties—studies on isolated hepatocytes and lipid membrane vesicles. *Hepatology* **4,** 661–666.

Skehan, P., Storeng, R., Scudiero, D., Monks, A., McMahon, J., Vistica, D., Warren, J. T., Bokesch, H., Kenney, S., and Boyd, M. R. (1990). New colorimetric cytotoxicity assay for anticancer-drug screening. *J. Natl. Cancer Inst.* **82,** 1107–1112.

Sodeman, T., Bronk, S. F., Roberts, P. J., Miyoshi, H., and Gores, G. J. (2000). Bile salts mediate hepatocyte apoptosis by increasing cell surface trafficking of Fas. *Am. J. Physiol. Gastrointest. Liver Physiol.* **278,** G992-G999.

Sokol, R. J., Winklhofer-Roob, B. M., Devereaux, M. W., and McKim, J. M., Jr. (1995). Generation of hydroperoxides in isolated rat hepatocytes and hepatic mitochondria exposed to hydrophobic bile acids. *Gastroenterology* **109,** 1249–1256.

Spivey, J. R., Bronk, S. F., and Gores, G. J. (1993). Glycochenodeoxycholate-induced lethal hepatocellular injury in rat hepatocytes. Role of ATP depletion and cytosolic free calcium. *J. Clin. Invest.* **92,** 17–24.

Stocchi, V., Cucchiarini, L., Magnani, M., Chiarantini, L., Palma, P., and Crescentini, G. (1985). Simultaneous extraction and reverse-phase high-performance liquid chromatographic determination of adenine and pyridine nucleotides in human red blood cells. *Anal. Biochem.* **146,** 118–124.

Yerushalmi, B., Dahl, R., Devereaux, M. W., Gumpricht, E., and Sokol, R. J. (2001). Bile acid-induced rat hepatocyte apoptosis is inhibited by antioxidants and blockers of the mitochondrial permeability transition. *Hepatology* **33,** 616–626.